

Dynamic monitoring of soil wind erosion in Inner Mongolia of China during 1985–2011 based on geographic information system and remote sensing

Yi Zhou¹ · Bing Guo^{1,2} · Shixin Wang¹ · Heping Tao³ · Wenliang Liu¹ · Guang Yang^{1,2} · Jinfeng Zhu¹

Received: 26 April 2014 / Accepted: 14 April 2015
© Springer Science+Business Media Dordrecht 2015

Abstract In Inner Mongolia, soil wind erosion is a serious environmental problem. The aim of the study was to develop an estimation model to analyze the spatial and temporal changes of soil wind erosion during 1985–2011 based on geographic information system and remote sensing. The results showed that wind erosion was widely distributed in Inner Mongolia with an area of approximately 95×10^4 km². During 1985–2011, wind erosion has deteriorated over the entire region of Inner Mongolia, which was indicated by enlarged zones of erosion at severe and intensive grades. There was a significant difference in change intensity among different plant types that zones occupied by barren or sparsely vegetation showed the severest deterioration while the wind erosion of cropland showed a slight improvement in wind erosion. In addition, a significantly negative relation was noted between change intensity of wind erosion and vegetation coverage. Furthermore, the change rate of wind erosion was negatively correlated with the number of days (wind velocity ≥ 6 m/s). The relationships between soil types and change intensity differed with the surface distributions of sandy, loamy and clayey soil with particle sizes of 0–1 cm. The soil type of haplic luvisols showed the strongest resistance to wind erosion. The results have certain significance for understanding the mechanism and change process of wind erosion and can provide a scientific basis for the prevention of wind erosion in Inner Mongolia.

Keywords Wind erosion · Estimation model · Inner Mongolia · Soil erodibility · Snow cover days · Aridity index

✉ Bing Guo
guobingjl@163.com

¹ Institute of Remote Sensing and Digital Earth, Chinese Academy of Science, Beijing 100094, China

² University of Chinese Academy of Sciences, Beijing 100049, China

³ Institute of Mountain Hazards and Environment, Chinese Academy of Sciences, Chengdu 610041, China

1 Introduction

Soil wind erosion is a natural geological process and comprises the detachment, movement and deposition of particles by wind (Zobeck 1991; Shi et al. 2003). Soil wind erosion has become a serious environmental problem throughout the world, which can lead to changes in global biochemical cycles and agricultural productivity decline, especially in arid and semi-arid regions. (Wang 2000). Rapid industrialization and urbanization have largely contributed to the eco-environmental deterioration (Cesari et al. 2012). China is one of the countries suffering the most serious soil wind erosion, with 60.9 % of its territories under the influence of wind erosion (Li et al. 2002a).

During the past decades, global warming has exerted significant impacts on terrestrial ecosystems and the impacts have been projected to be greater in the future (Gong and Shi 2003; Fu et al. 2007). Continuously rising temperatures and decreased precipitation have significantly exacerbated the process of wind erosion in arid and semi-arid regions, particularly in Inner Mongolia of China (Li et al. 2000, 2002b). According to the second national soil erosion remote sensing survey, wind erosion is severe in Inner Mongolia because of natural hazards (drought and sandstorm) and human activities (Nakano et al. 2008). The evaluation of soil wind erosion can provide basic data and information for the sustainable development. Therefore, an accurate estimation of wind erosion in Inner Mongolia is urgent for ecological and environmental protection.

However, a lack of accurate information on such factors as metrological data and soil types leads to a critical limitation in the study of large-scale wind erosion (Jiang et al. 2003; Sharratt and Edgar 2011). Quantifying the soil wind erosion is difficult although most of the previous field observations have facilitated the estimation of wind erosion

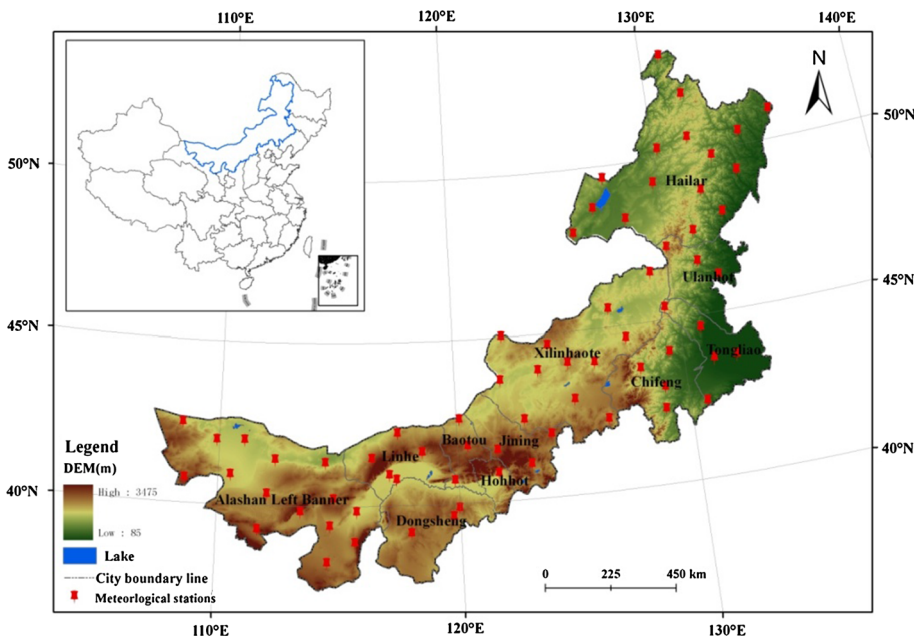


Fig. 1 Location of Inner Mongolia and the digital elevation model (DEM)

(Feng and Sharratt 2007; Korcz et al. 2009). Currently, systematic research in this regard is mostly at the macro-level and focuses on natural conditions of wind erosion, sandstorm activities and regular sandstorm movement (McHenry and Ritchie 1977; Steffens et al. 2008; Wang 2000; Zhang et al. 2003; Buschiazzo and Zobeck 2008). Previous studies were mostly based on site surveys, fixed position observations and experiments, which were conducted to simulate the process of soil wind erosion (Bilbro and Fryrear 1994; Fister and Ries 2009; Thorne et al. 2003; Verheijen et al. 2009). Recently, geographic information system (GIS) and remote sensing (RS) have been used as powerful tools for the evaluation of soil wind erosion. Satellite images are especially of great importance in providing frequent information of inaccessible area (Zobeck et al. 2000; Zhang et al. 2012). Thus, the integration of GIS and RS can provide an excellent platform for data capture, synthesis and analysis (Zhao et al. 2006). In this paper, the spatial and temporal patterns of change intensity of wind erosion were analyzed under the support of GIS and RS for the past 27 years (1985–2011).

2 Data and methodology

2.1 Study area

Inner Mongolia is located in northern China (36°–53°N, 105°–136°E) with an area of 1.18×10^6 km² (Hoffmann et al. 2008; Fig. 1). Most of the regions have at least 1000 m altitude. The annual average temperature ranges from –1 to 10 °C, decreasing from lower to higher altitudes (Jiang et al. 2003). Precipitation decreases from more than 450 mm in the east to 50 mm in the west, with approximately 80 % occurring in the growing season from May to September. In the western part of Inner Mongolia, vegetation coverage and biomass production are lower due to scarce precipitation. According to the US Department of Agriculture soil classification (Zhang et al. 2008), the major soil types in Inner Mongolia are sandy clay loam, clay loam and sandy loam.

2.2 Evaluation factors

There are many factors that affect the process of soil wind erosion, including climate factors and vegetation coverage. It is essential to select appropriate factors for the estimation of soil wind erosion. It is true that the complexity of the wind erosion model is borne from the fact that the factors controlling soil wind erosion vary in degree of influence through space and time. In order to synthetically analyze the changes of wind erosion, we selected five critical parameters including the number of snow cover days (Webb et al. 2009), soil erodibility (Miao et al. 2004), aridity index (Chung et al. 2013), vegetation fraction (Feng and Sharratt 2007) and annual average wind velocity (Grini and Zender 2004) after the observation of a field work by fully considering the loose soil surface, widely distributed desert, strong winds and low vegetation coverage in Inner Mongolia. With the support of ArcGIS software, all data were projected using the Arbers projection and were transferred to 1 km × 1 km raster data.

Due to great differences and different units among all the evaluating factors, it was difficult to evaluate the wind erosion intensity. The original values of each factor should be standardized to 0–1 by the following equations:

$$\text{Positive factor: } I_{ij} = \frac{x_{ij} - x_{\min,j}}{x_{\max,j} - x_{\min,j}} \quad (1)$$

$$\text{Negative factor: } I_{ij} = \frac{x_{\max,j} - x_{ij}}{x_{\max,j} - x_{\min,j}} \quad (2)$$

where I_{ij} represents the standardized value of grid i in factor j ; x_{ij} is the original value of grid i in factor j ; $x_{\max,j}$ and $x_{\min,j}$ represent the maximum and minimum values of factor j , respectively.

2.2.1 Number of snow cover days

The climate of Inner Mongolia is significantly affected by the cold current of Mongolia–Siberian system. The snow days often last for more than 3 months, and the annual average snow depth can reach 10–15 cm (Jiang et al. 2003). Accumulated snow can significantly reduce the area of the top layer of soil exposed to the wind. Wind erosion does not occur when the fraction of snow cover reaches 60 % (Wei et al. 2002). Moreover, the water saturation of the shallow surface soil, resulted from the melted snow, can rearrange the physical structure of soil particles. Then, the process can change the soil bulk permeability, which increases the stability of the surface soil (Fan et al. 2007; Qi et al. 2008). The snow cover products can be obtained using the satellite reflectance data, such as MODIS bands 4 (0.545–0.565 μm) and 6 (1.628–1.652 μm) (Salomonson and Appel 2004; Hall and Riggs 2007). However, in this paper, we utilized the field observations to calculate the factor of snow cover day, fully considering the deficiencies in spatial resolution and accuracy of the results that derived from remote sensing data. The daily meteorological observations for Inner Mongolia comprise snow depth, daily average/maximum/minimum temperature and precipitation, provided by the China Meteorological Administration (CMA). To calculate the number of snow cover days, we used the data from 236 meteorological stations in and around Inner Mongolia recorded during 1985–2011. A snow cover day was defined as that when the snow depth reached 0.5 cm.

2.2.2 Soil erodibility

Soil erodibility, a complex property that is determined by a wide of interlinked parameters, is an essential parameter required for the prediction of soil erosion (Bryan 1968; Geeves et al. 2000). It can better indicate the soil's resistance to dispersion and suspension in water or wind disturbance (Raupach and Lu 2004). Moreover, soil erodibility is associated with several parameters such as soil structure, organic content, surface roughness and soil texture (Cohen et al. 2005). It is generally considered as an inherent soil property with a constant value for a given soil type (Webb et al. 2009). The direct measurements of soil erodibility require long-term erosion plot studies, which are time-consuming and costly. Most of the previous equations require relatively large number of specific physical soil properties that are not widely available (Shao et al. 2002; Zhang et al. 2006). The soil erodibility factor (I) of wind erosion prediction models (WEPS) is a measure of the potential soil loss from a wide, bare, smooth, unsheltered surface (Wagner 2013). However, the interaction of the soil erodibility factor (I) and wind field intensity cannot be addressed in WEPS (Chung et al. 2013). The wind critical velocity is significantly influenced by the physical structure of soil, roughness and soil texture. Soil erodibility is

generally thought to be a consequence of fine particles (silt, clay and sand) and soil nutrients (organic C). Thus, the interaction can be considered to some extent.

In this study, the data of soil organic carbon and soil particle size distribution, obtained from the Institute of Soil Science, Chinese Academy of Sciences, were used to calculate soil erodibility:

$$SE = \left\{ 0.2 + 0.3 \exp \left[-0.0256 S_a \left(1 - \frac{S_i}{100} \right) \right] \right\} \times \left(\frac{S_i}{C_l + S_i} \right)^{0.3} \times \left[1 - \frac{0.25C}{C + \exp(3.72 - 2.95C)} \right] \times \left[1 - \frac{0.7S_n}{S_n + \exp(-5.51 - 22.9S_n)} \right] \tag{3}$$

where SE is soil erodibility ($t \text{ ha h}^{-1} \text{ MJ}^{-1} \text{ mm}^{-1}$); S_a (0.05–2 mm), S_i (0.002–0.05 mm) and C_l (< 0.002 mm) refer to sand fraction (%), silt fraction (%) and clay fraction (%), respectively; C is the soil organic carbon content (%); and S_n is equal to $1 - S_a/100$.

2.2.3 Aridity index

The aridity index is a function of precipitation and reference evapotranspiration, which is often used as the representative indicator to estimate the impacts of climate variation on hydrological processes (Beier et al. 2004). It represents a considerable water deficit in the top layer of the soil (Rana et al. 2005). Wind can easily remove and transfer soil particles when the top layer of the soil is totally dry and has lost the water content necessary for bonding (Hagen 1991). In this study, aridity was calculated with daily meteorological data provided by CMA:

$$D = 0.16 \sum \geq 10^\circ C/P \tag{4}$$

where D is the aridity index $\sum \geq 10^\circ C$ refers to the sum of air temperature that is higher than $10^\circ C$ in 1 year and P is the sum of precipitation during the period in which the air temperature is higher than $10^\circ C$.

2.2.4 Annual average wind velocity

During the wind erosion period, the wind velocity is a main contributor to wind erosion, particularly in arid and semi-arid regions (Grini and Zender 2004). Soil wind erosion is largely affected by wind velocity and critical friction wind velocity on the ground surface (Li et al. 2003). Furthermore, wind speed has a positive relation with wind erosion. Wind can remove soil particles when the wind velocity reaches a certain critical speed. Many studies reported that the critical wind velocities were influenced by soil particle size, moisture content and hardness (Bryan 1968; Geeves et al. 2000; Chappell et al. 2006). In Inner Mongolia, the strong winds are usually brought by the cold current of Mongolian–Siberian system in spring and winter. In this study, the annual average wind velocity was calculated based on the daily meteorological data provided by CMA.

2.2.5 Vegetation fraction

Green vegetation cover on the land surface is of great importance in regulating surface wind and hydrological processes because it can mitigate the erosion forces of wind and

rainfall (Duan et al. 2006; Chen et al. 2007). Impacts of soil and vegetation properties on the soil wind erosion are attributed to their influences on surface roughness length (Rau-pach and Lu 2004). Furthermore, soil coverage is a key factor to estimate the wind erosion intensity (Wagner 2013). However, this factor is difficult to obtain through the tools of remote sensing because the components of the terrestrial eco-system are very complicated. But, in Inner Mongolia, a pixel can be defined as the combination of the bare soil and pure vegetation (Zhao et al. 2006). We utilized the index of vegetation coverage to replace the parameter of soil coverage. The Normalized Difference Vegetation Index (NDVI; Huete and Tucker 1991), a better indicator of the vegetation grown, has been employed to calculate vegetation coverage. In this paper, the dimidiated pixel model was utilized to obtain the vegetation fraction, which could eliminate the influence of clouds and soil background:

$$VF = \frac{ndvi - ndvi_{soil}}{ndvi_{veg} - ndvi_{soil}} \quad (5)$$

where VF represents the vegetation fraction; $ndvi$ is value of each pixel; $ndvi_{soil}$ represents the minimum value of all pixels at the confidence of 0.005; $ndvi_{veg}$ represents the maximum value of all pixels at the confidence of 0.995.

The time-series NDVI data of 1985 were derived from the Advanced Very High Resolution Radiometer (AVHRR), available at <http://daac.gsfc.nasa.gov/>, at 8 km spatial resolution with a 15-day interval. The spatial resolution of moderate resolution imaging spectroradiometer (MODIS) NDVI of 2011 was 1 km \times 1 km, produced by the National Aeronautics and Space Administration (NASA) Earth Observing System. To confirm the spatial resolution consistency of the two datasets, the GIMMS NDVI data were converted into grid cells at a resolution of 1 km \times 1 km by using the nearest neighbor assignment resampling algorithm with ArcGIS 10.1. Then, the monthly NDVI data were produced by the maximum-value composition technique to minimize the effects of atmospheric effects and solar zenith angle (Stow et al. 2004). Finally, the average annual vegetation cover was obtained on the basis of the monthly NDVI data.

2.3 Evaluation model of wind erosion

Evaluation of wind erosion requires integration of multiple factors to obtain a comprehensive index. Thus, the method of weighted linear combinations was adopted to calculate the SWEI.

$$SWEI = \frac{\sum_{i=1}^n W_i I_i}{\sum_{i=1}^n W_i} \quad (6)$$

where SWEI is the soil wind erosion index; W_i refers the weight of factor i ; and I_i refers the value of factor i .

Another important issue for the evaluation was to assign weight to each factor according to its relative effects on the environmental vulnerability. The analytic hierarchy process (AHP) (Shi et al. 2003) was an appropriate method for deriving the weight assigned to each factor. AHP had been widely applied in environmental evaluation and regional sustainable management (Korczy et al. 2009). The relative importance of the five factors was obtained

with field investigations and expert knowledge. In this paper, the process of obtaining the weight of each factor is shown in Table 1.

3 Results

3.1 Classification of wind erosion and accuracy assessment

The results obtained from SWEI model and AHP were continuous values, which should be classified into six levels standing for different erosion intensity. The classification is of great importance in the evaluation of soil wind erosion, so it should be objective and logical. The tool of histogram was often applied to explore the statistical distribution of the classes and clusters in the attribute space (Nakano et al. 2008). Thus, in this study, the natural breaks of ArcGis10.1 (Jenks 1967) that combined the methods of histogram and cluster had been applied to grade the vulnerability into six grades.

The six categories included no erosion ($I < 0.23$), slight erosion ($0.23 < I < 0.35$), mild erosion ($0.35 < I < 0.43$), moderate erosion ($0.43 < I < 0.50$), intensive erosion ($0.50 < I < 0.56$) and severe erosion ($0.56 < I$). The spatial patterns of wind erosion in 1985 and 2011 are shown in Fig. 2.

The basic error matrices (Bruin 2000) and the precision index were applied to test the accuracy of the estimated results. To confirm the validity of the sampling points in 2011, 285 sites (Table 2) were chosen from regions with different landforms, slopes, soil types and land-use types. The error matrix of the calculated erosion category and the field survey results are listed in Table 3.

In Table 3, the cartographic precisions of all categories ranged from 0.75 to 0.92. The classification results were in agreement with the actual erosion levels, which could be indicated by the significant credibility in the evaluation of the wind erosion. Moreover, slight erosion had the best evaluation precision, followed by intensive erosion while the accuracies of mild and moderate erosion were much lower. On the whole, the wind erosion model of Inner Mongolia was effective and accurate with an overall precision of 84.21 %.

3.2 Spatial differentiations and changes of wind erosion between 1985 and 2011

Through Fig. 2, it can be found that wind erosion was widely distributed in Inner Mongolia with an area of $95(10^4)$ km², covering approximately 86 % of the region. In detail, the main spatial patterns of soil wind erosion in Inner Mongolia were the contrast between the western parts and eastern parts. The eastern parts including Hailar and Ulanhot were

Table 1 Relative weights of factors for soil wind erosion evaluation

Factors	(1)	(2)	(3)	(4)	(5)	Weights
(1) Soil erodibility	1					0.139
(2) Annual average wind velocity	2	1				0.278
(3) Aridity index	1	1/2	1			0.156
(4) Number of snow cover days	1	1/2	1/2	1		0.105
(5) Vegetation faction	2	1	2	4	1	0.319

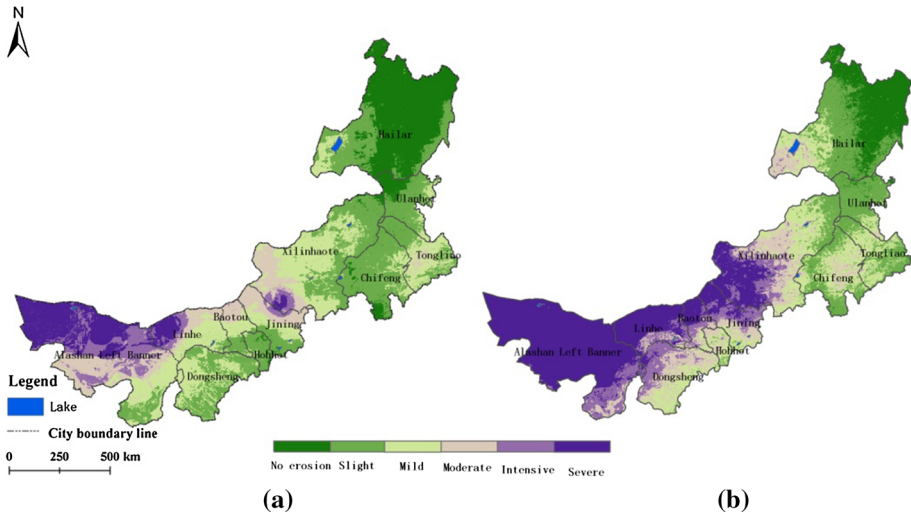


Fig. 2 Spatial distributions of wind erosion intensity in Inner Mongolia. **a** Grades of wind erosion in 1985; **b** grades of wind erosion in 2011

Table 2 Error matrix of wind erosion categories for 2011

Levels of sampling points in 2011	Wind erosion results evaluated in 2011					Sum
	Slight erosion	Mild erosion	Moderate erosion	Intensive erosion	Severe erosion	
Slight erosion	76	3	2	2	0	83
Mild erosion	5	63	2	3	2	75
Moderate erosion	4	5	36	3	0	48
Intensive erosion	1	0	3	42	3	49
Severe erosion	2	3	0	2	23	30
Sum	88	74	43	52	28	285

Table 3 Precision index of grades of wind erosion

Precision test	User accuracy	Commission	Cartographic accuracy	Omission
Slight erosion	0.86	0.14	0.92	0.08
Mild erosion	0.85	0.15	0.84	0.16
Moderate erosion	0.83	0.17	0.75	0.25
Intensive erosion	0.80	0.20	0.86	0.14
Severe erosion	0.82	0.18	0.77	0.23

mainly occupied by the zones of no, slight and mild erosion, while the severe and intensive erosion zones were distributed continuously in the mid-western region such as Alashan Left Banner and Linhe. Moderate and mild erosion zones were distributed between the zones of severe erosion and slight erosion.

In 1985, the slight erosion zone covered the largest region with the area of $36.57(10^4)$ km², accounting for 31.98 %. The zones of no, mild, moderate, intensive and severe erosion were $19.95(10^4)$, $27.44(10^4)$, $12.65(10^4)$, $7.27(10^4)$ and $10.46(10^4)$ km², respectively. However, in 2011, the zone of severe erosion covered the largest region with the area of $33.40(10^4)$ km², accounting for 29.25 %, followed by zones of slight [$22.82(10^4)$ km²] and mild [$20.10(10^4)$ km²] erosion.

During 1985–2011, there was a deterioration of wind erosion over the whole Inner Mongolia, as most of the no, slight, mild erosion zones had disappeared with a great increase in severe erosion (Table 4). In view of spatial distribution, the deteriorated regions were located in southern Alashan Left Banner, northern Dongsheng and western Xilinhaote while the zones of decreased erosion intensity were mainly distributed in eastern Ulanhot and eastern Tongliao.

To detect the detailed process of soil wind erosion change, the change matrix of wind erosion grades was conducted through the spatial overlay of the two maps of soil wind erosion grades. In view of the change matrix (Fig. 3), there was an aggravation of soil wind erosion for the entire study region during 1985–2011. As shown in Fig. 3, the detailed process of change for each grade of wind erosion was quite different, which could be characterized as follows: during 1985–2011, the severe erosion was the most stable grade with 72.40 % unchanged, followed by the grade of no erosion (52.57 %). Meanwhile, the grade of moderate erosion had the most dramatic change with only 15.32 % unchanged, while the rest mainly changed to be intensive and severe grades. There was 64.66 % of slight erosion turning to be higher grades of erosion with 32.55 % of this zone unchanged. The intensive erosion was the second most dramatic grade with 28.25 % unchanged while the rest mainly degraded to be slight erosion. Therefore, it was concluded that there was a deteriorated trend of soil wind erosion in Inner Mongolia during the study period.

3.3 Change intensity of wind erosion between 1985 and 2011

To more effectively monitor the changes of wind erosion, the change intensity (CI) of wind erosion between 1985 and 2011 was obtained by using the raster calculator of ArcGIS10.1. Based on the natural conditions in Inner Mongolia, the erosion change intensity was divided into six categories including moderate decrease (MD; $CI < -0.15$), slight decrease (SD; $-0.15 < CI < -0.05$), stable (ST; $-0.05 < CI < 0.05$), slight increase (SLI; $0.05 < CI < 0.15$), moderate increase (MI; $0.15 < CI < 0.25$) and intensive increase (II;

Table 4 Area and area ratios of different grades of wind erosion intensity in 1985 and 2011

Grades of wind erosion	1985		2011	
	Area/(10 ⁴) km ²	Area ratio/%	Area/(10 ⁴) km ²	Area ratio/%
No erosion	19.95	17.45	11.53	10.10
Slight erosion	36.57	31.98	22.82	19.98
Mild erosion	27.44	24.00	20.10	17.60
Moderate erosion	12.65	11.06	14.50	12.70
Intensive erosion	7.27	6.36	11.84	10.37
Severe erosion	10.46	9.15	33.40	29.25

Fig. 3 Change matrix of area ratios of different erosion intensities during 1985–2011. *NE* no erosion, *SLE* slight erosion, *MIE* mild erosion, *MOE* moderate erosion, *IE* intensive erosion, *SEE* severe erosion

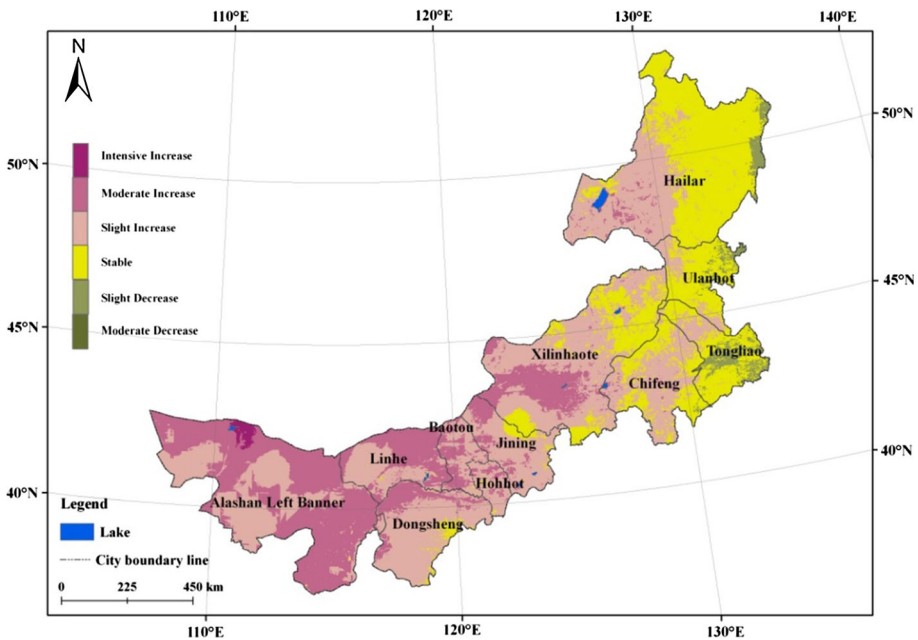
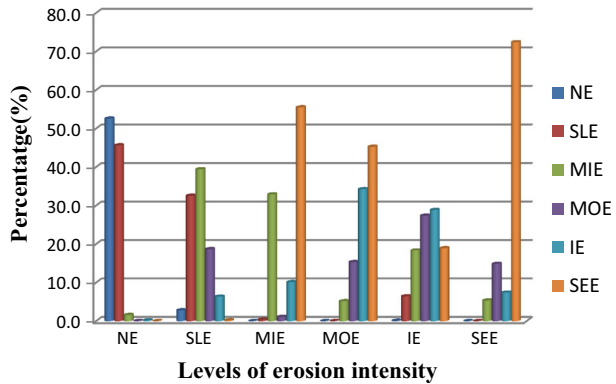


Fig. 4 Classification map of wind erosion change intensity during 1985–2011

0.25 < CI). As shown in Fig. 4, there was a distinct spatial differentiation of wind erosion for each grade of change intensity during 1985–2011. The slight increase was the most widely distributed grade with an area of $51.82(10^4)$ km², mainly occurred in mid-western regions such as Xilinhaote, Jining and Dongsheng. The moderate increase was the second most widely distributed grade with the area of $28.09(10^4)$ km², including Alashan Left Banner and Linhe. The eastern Inner Mongolia was mainly occupied by the stable [$21.81(10^4)$ km²] and slight decrease [$9.10(10^4)$ km²] zones. Therefore, it was proved that during 1985–2011, wind erosion had deteriorated over the entire region of Inner Mongolia.

4 Discussions

4.1 Improvement of the model for wind erosion

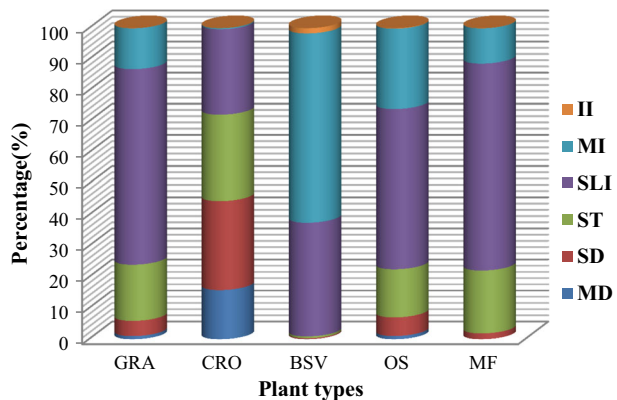
Inner Mongolia is one of the major wind erosion regions in China. However, compared with the soil water erosion, studies on wind erosion of this region based on GIS and RS are fewer.

In this paper, five critical factors on wind erosion occurrence and development were chosen to obtain the comprehensive evaluation of wind erosion, which consisted of the number of snow cover days, soil erodibility, aridity index, vegetation fraction and annual average wind velocity. All the factors could better reflect the process of the wind erosion in Inner Mongolia. The results of the accuracy assessment indicated that the evaluation model of wind erosion was effective and had better applicability in Inner Mongolia. Moreover, it was convenient for us to obtain the dynamic information of wind erosion in large-scale region.

4.2 Relationship between change intensity of wind erosion and vegetation variables

Wind erosion control effectively depends on the plant types and management system (Fu et al. 2007). In order to explore the relationship between the change intensity and plant types, we chose five typical plant types, i.e., grassland, cropland, barren or sparsely vegetation, open shrubs and mingled forest. As shown in Fig. 5, there was a significant difference in change intensity among different plant types. By comparing the area ratios of change intensity grades in each plant type, it could be found that the grassland, open shrubs and mingled forest were mainly occupied by the zones of slight increase and stable, while intensive increase zone only accounts for 5 % of each plant type. During 1985–2011, it showed a deteriorated trend of wind erosion in grassland, mingled forest and barren or sparsely vegetation. This was because that the barren or sparsely vegetation was widely distributed in western part of Inner Mongolia with rare precipitation. Moreover, during the past decades, the global warming has accelerated, resulting in increased temperature and decreased rainfall (Li et al. 2002a). The vegetation coverage and soil moisture both had been negatively influenced by the process of climate change, which could significantly

Fig. 5 Area percentages of different grades of change intensity for each plant type during 1985–2011. *GRA* grassland, *CRO* cropland, *BSV* bare or sparsely vegetation, *OS* open shrubs, *MF* mingled forest, *MD* moderate decrease, *SD* slight decrease, *ST* stable, *SLI* slight increase, *MI* mild increase, *II* intensive increase



control the process of soil wind erosion. Thus, soil wind erosion of zones occupied by barren or sparsely vegetation has aggravated during 1985–2011. However, along with the decreased precipitation, human activities such as deforestation and overgrazing exerted great influences on eco-environment of zones dominated by grassland and mingled forest (Hoffmann et al. 2008). These activities would destroy the vegetation cover and physical structure of the top soil. Therefore, both natural and anthropogenic factors would aggravate the process of wind erosion in regions occupied by grassland and mingled forest. However, it showed a wind erosion improvement in open shrubs and cropland because of the abundant precipitation (300–400 mm) and anthropogenic management (Li et al. 2002b). Furthermore, data of 52 sampling points (Fig. 1) were utilized to examine the relation between change intensity and vegetation coverage. Figure 6 shows that the change intensity and vegetation coverage had a negative relationship, which was indicated by the trend coefficient of -0.1828 .

4.3 Relationship between change intensity of wind erosion and wind field intensity

Wind speed has a positive relation with wind erosion, and wind can remove soil particles when the wind velocity reaches a certain critical speed of 6 m/s (Fister and Ries 2009). Therefore, in order to analyze how the wind field intensity affected the process of the soil wind erosion, we calculated the number of days when the daily average wind velocity reached 6 m/s ($WV \geq 6$ m/s) based on 52 meteorological stations (Fig. 1). Figure 7 showed that the soil wind erosion intensity would aggravate with the enlarged number of days ($WV \geq 6$ m/s), which was indicated by the positive value of the change intensity. However, the change rate of the soil wind erosion became smaller with the increased number of days ($WV \geq 6$ m/s). Furthermore, the change rate became a constant while the number of days ($WV \geq 6$ m/s) reached 50. These phenomena occurred because the degree of wind erosion intensity was restrained by the rare occurrence of soil in regions with strong winds and the ground was always covered with bare rock and gravel (Zhang et al. 2008).

4.4 Relationship between change intensity of wind erosion and soil types

In this section, six typical soil types were selected to explore the relation between change intensity of wind erosion and soil types. These soil types included calcic chernozems (CC),

Fig. 6 Linear relation between change intensity and vegetation coverage. *CI* change intensity, *VC* vegetation coverage

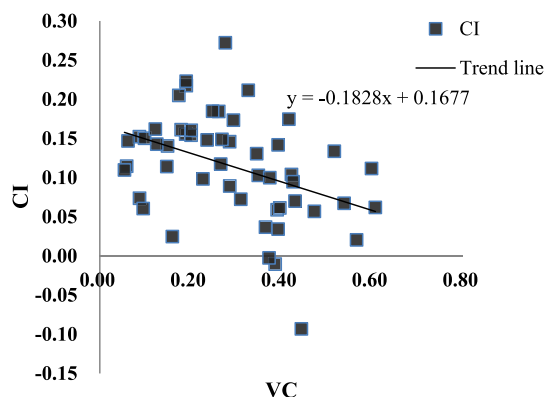


Fig. 7 Linear relation between change intensity and number of days (wind velocity ≥ 6 m/s). *CI* change intensity, *NDWV* (≥ 6 m/s), number of days (wind velocity ≥ 6 m/s)

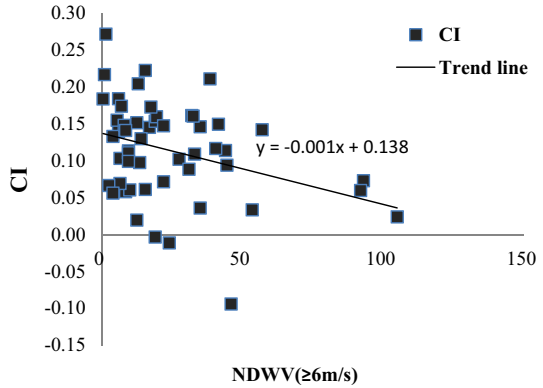
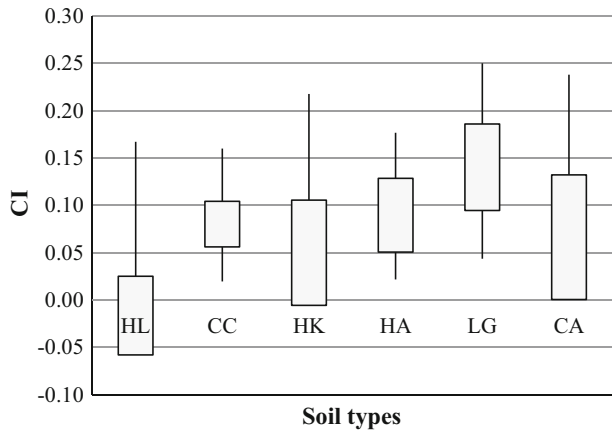


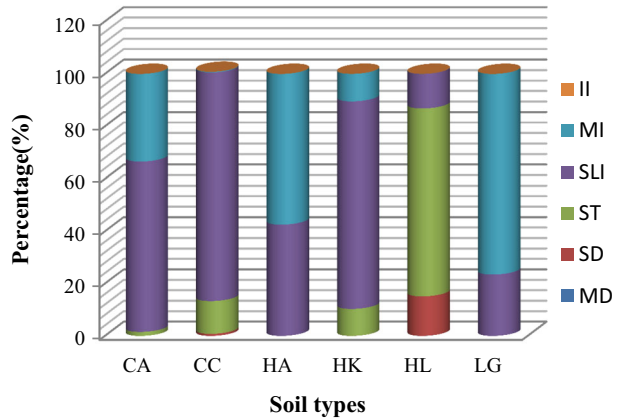
Fig. 8 The change intensity of wind erosion for each soil type. The *top* of each *line* represents the maximum value of erosion change intensity for each soil type, while the *bottom* of *box* shows the minimum value. The *top* of the *box* refers to the mean value of change intensity, and the length of *box* refers to the standard deviation of erosion change intensity



calcaric arenosols (CA), luvic gypsisols (LG), haplic luvisols (HL), haplic arenosols (HA) and haplic kastanozems (HK).

Figure 8 showed that there was a significant difference in change intensity of wind erosion among the soil types. In view of mean change intensity, LG had the largest value of 0.186 that belonged to the grade of moderate increase, followed by CA and HA, while the HL had the smallest value of 0.025. Attempts had been made to confirm that soil erodibility, affected by the inherent properties of the soil, reflected the vulnerability of the soil itself to erosion (Zhou and Wu 1993; Miao et al. 2004). In addition, CaCO_3 in top layer of the soil could cement soil particles to form large clumps, which largely decreased the soil erodibility (Zhao and Shi 2003). Therefore, the change intensities of CC, HL and HK were significantly smaller than those of LG and CA. Previous studies also found that the surface distributions of different soil types with particle sizes of 0–1 cm were important for determining soil erodibility (Miao et al. 2004). Under the same conditions, the critical wind velocity for wind erosion of sandy soil was larger than that of loamy soil. Moreover, soil erodibility decreased with an increase in soil particles size (Vaezi et al. 2008). By comparing the area percentages of change intensity grades in each soil type (Fig. 9), it could be found that CA, CC, HK and LG were mainly occupied by grades of slight and moderate

Fig. 9 Area percentages of different grades of change intensity for each soil type during 1985–2011. *CA* calcareic arenosols, *CC* calcic chernozems, *HA* haplic arenosols, *HK* haplic kastanozems, *HL* haplic luvisols, *LG* luvisols



increase, while HL was dominated by grade of stable. Thus, it could be concluded that HL showed the strongest resistance to wind erosion.

5 Conclusions

Soil wind erosion, as a main contributor to deterioration of eco-environment, can significantly threaten the sustainable development of rural areas. Inner Mongolia is a typical semi-arid and arid region, which is greatly affected by the soil wind erosion. This study developed a new estimation model of wind erosion with strong operability and practicability under the support of GIS and RS.

This study demonstrated that wind erosion was widely distributed in Inner Mongolia with an area of approximately $95(10^4)$ km², accounting for 86 % of the study region. The western Inner Mongolia was mainly occupied by the grades of intensive and severe erosion, whereas the east parts were dominated by grades of no, slight and mild erosion. During 1985–2011, there was a deterioration of wind erosion over the whole Inner Mongolia, which was indicated by enlarged zones of severe, intensive erosion. Our study revealed that the vegetation coverage had a negative relationship with change intensity of wind erosion and zones occupied by barren or sparsely vegetation were the most severely deteriorated region, while the soil wind erosion of cropland showed a slight improvement during 1985–2011. In addition, the change rate of wind erosion had a negative relation with the number of days ($WV \geq 6$ m/s). The relations between soil types and change intensity differed with the content of CaCO₃ and the surface distributions of sandy, loamy and the clayey soil with particle sizes of 0–1 cm. However, the factors of the evaluation obtained by GIS and RS should be improved, and the quantitative relations between the factors and soil wind erosion should be clarified in further studies.

Acknowledgments This work was supported by Foundation of Director of Institute of Remote Sensing and Digital Earth, Chinese Academy of Science (No. Y4SY0200CX) and Special Project on High Resolution of Earth Observation System for Major Function Oriented Zones Planning (No. 00-Y30B14-9001-14/16).

References

- Beier C, Emmett B, Gundersen P et al (2004) Novel approaches to study climate change effects on terrestrial ecosystems in the field: drought and passive nighttime warming. *Ecosystems* 7(6):583–597. doi:[10.1007/s10021-004-0178-8](https://doi.org/10.1007/s10021-004-0178-8)
- Bilbro JD, Fryrear DW (1994) Wind erosion losses as related to plant silhouette and soil cover. *Agron J* 86(3):550–553
- Bruin S (2000) Predicting the areal extent of land-cover types using classified imagery and geostatistics. *Remote Sens Environ* 74(3):387–396. doi:[10.1016/S0034-4257\(00\)00132-2](https://doi.org/10.1016/S0034-4257(00)00132-2)
- Bryan RB (1968) The development, use and efficiency of indices of soil erodibility. *Geoderma* 2(3):5–26
- Buschiazzo DE, Zobeck TM (2008) Validation of WEQ, RWEQ and WEPS wind erosion for different arable land management systems in the Argentinean Pampas. *Earth Surf Proc Land* 33(12):1839–1850. doi:[10.1002/esp.1738](https://doi.org/10.1002/esp.1738)
- Cesari D, Contini D, Genga A et al (2012) Analysis of raw soils and their re-suspended PM₁₀ fractions: characterisation of source profiles and enrichment factors. *Appl Geochem* 27(6):1238–1246. doi:[10.1016/j.apgeochem.2012.02.029](https://doi.org/10.1016/j.apgeochem.2012.02.029)
- Chappell A, Zobeck TM, Brunner G (2006) Using bi-directional soil spectral reflectance to model soil surface changes induced by rainfall and wind-tunnel abrasion. *Remote Sens Environ* 102(3–4):328–343. doi:[10.1016/j.rse.2006.02.020](https://doi.org/10.1016/j.rse.2006.02.020)
- Chen SQ, Wang LJ, Lv SH et al (2007) Study of NDVI and climate change in Maqu County, upstream of Yellow river. *J Glaciol Geocryol* 29(1):131–136 (in Chinese)
- Chung SH, Herron-Thorpe FL, Lamb BK et al (2013) Application of the wind erosion prediction system in the airport regional air quality modeling framework. *Trans Asabe* 56(2):625–641
- Cohen MJ, Shepherd KD, Walsh MG (2005) Empirical reformulation of the universal soil loss equation for erosion risk assessment in a tropical watershed. *Geoderma* 124(3–4):235–252. doi:[10.1016/j.geoderma.2004.05.003](https://doi.org/10.1016/j.geoderma.2004.05.003)
- Duan AM, Wu GX, Zhang Q (2006) New proofs of the recent climate warming over the Tibetan Plateau as a result of the increasing greenhouse gases emissions. *Chin Sci Bull* 51(11):1396–1400. doi:[10.1007/s11434-006-1396-6](https://doi.org/10.1007/s11434-006-1396-6)
- Fan L, Liu S, Bernhofer C et al (2007) Regional land surface energy fluxes by satellite remote sensing in the Upper Xilin River Watershed (Inner Mongolia, China). *Theor Appl Climatol* 88(3–4):231–245. doi:[10.1007/s00704-006-0241-9](https://doi.org/10.1007/s00704-006-0241-9)
- Feng G, Sharratt B (2007) Scaling from field to region for wind erosion prediction using the Wind Erosion Prediction System and graphical information systems. *Appl Res* 62(5):321–328 (In Chinese)
- Fister W, Ries JB (2009) Wind erosion in the Central Ebro Basin under changing land use management. Field experiments with a small, portable wind tunnel. *J Arid Environ* 73(11):996–1004. doi:[10.1016/j.jaridenv.2009.05.006](https://doi.org/10.1016/j.jaridenv.2009.05.006)
- Fu XF, Yang ST, Liu CM (2007) Changes of NDVI and their relations with principal climatic factors in the Yarlung Zangbo River Basin. *Geographic Research* 26(1):60–66 (In Chinese)
- Geeves GW, Leys JF, McTainsh GH (2000) Soil Erodibility. In: Charman PEV, Murphy BW (eds) *Soils: their properties and management*. Oxford University Press, New York, pp 205–220
- Gong DY, Shi PJ (2003) Northern hemispheric NDVI variations associated with large-scale climate indices in spring. *Int J Remote Sens* 24(12):2559–2566. doi:[10.1080/0143116031000075107](https://doi.org/10.1080/0143116031000075107)
- Grini A, Zender CS (2004) Roles of saltation, sandblasting, and wind speed variability on mineral dust aerosol size distribution during the Puerto Rican Dust Experiment (PRIDE). *J Geophys Res* 109(7):102–108. doi:[10.1029/2003JD004233](https://doi.org/10.1029/2003JD004233)
- Hagen LJ (1991) A wind erosion prediction system to meet users needs. *J Soil Water Conserv* 46(2):106–111
- Hall DK, Riggs GA (2007) Accuracy assessment of the MODIS snow products. *Hydrol Process* 21(12):1534–1547. doi:[10.1002/hyp.6715](https://doi.org/10.1002/hyp.6715)
- Hoffmann C, Funk R, Li Y et al (2008) Effect of grazing on wind driven carbon and nitrogen ratios in the grasslands of Inner Mongolia. *Catena* 75(2):182–190. doi:[10.1016/j.catena.2008.06.003](https://doi.org/10.1016/j.catena.2008.06.003)
- Huete AR, Tucker CJ (1991) Investigation of soil influences in AVHRR red and near infrared vegetation index imagery. *Int J Remote Sens* 12(6):1223–1242
- Jenks GF (1967) The data model concept in statistical mapping. *Int Yearbook Cartogr* 7:186–190
- Jiang DM, Liu ZM, Cao CY et al (2003) Desertification and ecological restoration of Horqin sandy land. China Environmental Science Press, Beijing, pp 32–142
- Korcz MJ, Fudala Klis C (2009) Estimation of wind blown dust emissions in Europe and its vicinity. *Atmos Environ* 43(7):1410–1420. doi:[10.1016/j.atmosenv.2008.05.027](https://doi.org/10.1016/j.atmosenv.2008.05.027)

- Li SG, Harazono Y, Oikawa T et al (2000) Grassland desertification by grazing and the resulting micrometeorological changes in Inner Mongolia. *Agric For Meteorol* 102(2–3):125–137. doi:[10.1016/S0168-1923\(00\)00101-5](https://doi.org/10.1016/S0168-1923(00)00101-5)
- Li FR, Zhao AF, Zhou HY et al (2002a) Effects of simulated grazing on grown and persistence of *Artemisia frigida* in a semiarid sandy rangelands. *Grass Forage Sci* 57(3):239–247. doi:[10.1046/j.1365-2494.2002.00322.x](https://doi.org/10.1046/j.1365-2494.2002.00322.x)
- Li LH, Han XG, Wang QB et al (2002b) Correlations between plant biomass and soil respiration in a *Leymus chinensis* community in the Xilin River Basin of Inner Mongolia. *Acta Bot Sin* 44(5):593–597 (**In Chinese**)
- Li FR, Zhang H, Zhang TH et al (2003) Variations of sand transportation rates in sandy grasslands along a desertification gradient in northern China. *Catena* 53(3):257–276. doi:[10.1016/S0341-8162\(03\)00039-0](https://doi.org/10.1016/S0341-8162(03)00039-0)
- McHenry JR, Ritchie JC (1977) Physical and chemical parameters affecting transport of CS₂-137 in arid watersheds. *Water Resour Res* 13(6):923–927. doi:[10.1029/WR013i006p00923](https://doi.org/10.1029/WR013i006p00923)
- Miao CY, He BH, Chen XY et al (2004) Analysis on correlativity of soil erodibility factors of USLE and WEPP models. *Soil Water Conserv China* 6(5):23–26 (**In Chinese**)
- Nakano T, Nemoto M, Shinoda M (2008) Environmental controls on photosynthetic production and ecosystem respiration in semi-arid grasslands of Mongolia. *Agric For Meteorol* 148(10):1456–1466. doi:[10.1016/j.agrformet.2008.04.011](https://doi.org/10.1016/j.agrformet.2008.04.011)
- Qi J, Ma W, Song CX (2008) Influence of freeze–thaw on engineering properties of a silty soil. *Cold Reg Sci Technol* 53(3):397–404. doi:[10.1016/j.coldregions.2007.05.010](https://doi.org/10.1016/j.coldregions.2007.05.010)
- Rana G, Katerji N, Lorenzi F (2005) Measurement and modelling of evapotranspiration of irrigated citrus orchard under Mediterranean conditions. *Agric For Meteorol* 128(3–4):199–209. doi:[10.1016/j.agrformet.2004.11.001](https://doi.org/10.1016/j.agrformet.2004.11.001)
- Raupach MR, Lu H (2004) Representation of land-surface processes in aeolian transport models. *Environ Model Softw* 19(2):93–112. doi:[10.1016/S1364-8152\(03\)00113-0](https://doi.org/10.1016/S1364-8152(03)00113-0)
- Salomonson VV, Appel I (2004) Estimating fractional snow cover from MODIS using the normalized difference snow index. *Remote Sens Environ* 89(3):351–360. doi:[10.1016/j.rse.2003.10.016](https://doi.org/10.1016/j.rse.2003.10.016)
- Shao YH, Jung E, Leslie LM (2002) Numerical prediction of northeast Asian dust storms using an integrated wind erosion modeling system. *J Geophys Res Atmos* 107(24):35–43. doi:[10.1029/2001JD001493](https://doi.org/10.1029/2001JD001493)
- Sharratt BS, Edgar R (2011) Implications of changing PM10 air quality standards on Pacific Northwest communities affected by windblown dust. *Atmos Environ* 45(27):4533–4814. doi:[10.1016/j.atmosenv.2011.05.059](https://doi.org/10.1016/j.atmosenv.2011.05.059)
- Shi TG, Sun XH, Yan BC (2003) Study on the seasonal wind–sand land in the Northwest Region of Shandong Province based on remote sensing. *Areal Res Develop* 22(5):43–45 (**In Chinese**)
- Steffens M, Kölbl A, Totsche KU et al (2008) Grazing effects on soil chemical and physical properties in a semiarid steppe of Inner Mongolia (PR China). *Geoderma* 143(1–2):63–72. doi:[10.1016/j.geoderma.2007.09.004](https://doi.org/10.1016/j.geoderma.2007.09.004)
- Stow DA, Hope A, MacGuire D et al (2004) Remote sensing of vegetation and land-cover change in Arctic Tundra Ecosystems. *Remote Sens Environ* 89(3):281–308. doi:[10.1016/j.rse.2003.10.018](https://doi.org/10.1016/j.rse.2003.10.018)
- Thorne ME, Young FI, Pan WI et al (2003) No-till spring cereal cropping systems reduce wind erosion susceptibility in the wheat-fallow region of the Pacific Northwest. *J Soil Water Conserv* 58(5):251–257 (**In Chinese**)
- Vaezi AR, Sadeghi SRH, Bahami HA et al (2008) Modeling the USLE K factor for calcareous soils in northwest Iran. *Geomorphology* 97(3–4):414–423. doi:[10.1016/j.geomorph.2007.08.017](https://doi.org/10.1016/j.geomorph.2007.08.017)
- Verheijen FGA, Jones RJA, Rickson RJ et al (2009) Tolerable versus actual soil erosion rates in Europe. *Earth Sci Rev* 94(1–4):23–38. doi:[10.1016/j.earscirev.2009.02.003](https://doi.org/10.1016/j.earscirev.2009.02.003)
- Wagner LE (2013) A history of wind erosion prediction models in the United States Department of Agriculture: the wind erosion prediction system (WEPS). *Aeolia Res* 10:9–24. doi:[10.1016/j.aeolia.2012.10.001](https://doi.org/10.1016/j.aeolia.2012.10.001)
- Wang T (2000) Land use and sandy desertification in the North China. *J Des Res* 20(2):103–107 (**In Chinese**)
- Webb NP, McGowan HA, Phinn SR et al (2009) A model to predict land susceptibility to wind erosion in western Queensland, Australia. *Environ Model Softw* 24(2):214–227. doi:[10.1016/j.envsoft.2008.06.006](https://doi.org/10.1016/j.envsoft.2008.06.006)
- Wei ZG, Huang RH, Chen W et al (2002) Spatial distributions and interdecadal variations of the snow at the Tibetan Plateau weather stations. *Chin J Atmos Sci* 26(4):496–508 (**In Chinese**)
- Zhang CL, Gong JR, Zou XY et al (2003) Estimates of soil movement in a study area in Gonghe Basin, Northeast of Qinghai–Tibet Plateau. *J Arid Environ* 53(3):283–285. doi:[10.1006/jare.2002.1048](https://doi.org/10.1006/jare.2002.1048)

- Zhang HB, Luo YM, Zhao QG et al (2006) Hong Kong soil researches integrated evaluation of soil fertility quality based on the improved analytic hierarchy process. *Acta Pedol Sin* 43(4):577–583 **(In Chinese)**
- Zhang KL, Shu AP, Xu XL et al (2008) Soil erodibility and its estimation for agricultural soils in China. *J Arid Environ* 72(6):1002–1011. doi:[10.1016/j.jaridenv.2007.11.018](https://doi.org/10.1016/j.jaridenv.2007.11.018)
- Zhang ZD, Wieland R, Reiche M et al (2012) Identifying sensitive areas to wind erosion in the Xilingele grassland by computational fluid dynamics modeling. *Ecol Inform* 8:37–47. doi:[10.1016/j.ecoinf.2011.12.002](https://doi.org/10.1016/j.ecoinf.2011.12.002)
- Zhao XG, Shi H (2003) Prescription of soil anti-erosion capability under water erosion. *Arid Land Geogr* 26(1):12–16 **(In Chinese)**
- Zhao HL, Zhou RL, Zhang TH et al (2006) Effects of desertification on soil and crop growth properties in Horqin sandy cropland of Inner Mongolia, north China. *Soil Tillage Res* 87(2):175–185. doi:[10.1016/j.still.2005.03.009](https://doi.org/10.1016/j.still.2005.03.009)
- Zhou PH, Wu CL (1993) The research method of soil anti-scourability experiment on the Loess Plateau. *J Soil Water Conserv* 7(1):29–34 **(In Chinese)**
- Zobeck TM (1991) Soil properties affecting wind erosion. *J Soil Water Conserv* 46(2):112–118
- Zobeck TM, Parker NC, Haskell S et al (2000) Scaling up from field to region for wind erosion prediction using a field-scale wind erosion model and GIS. *Agric Ecosyst Environ* 82(1–3):247–259. doi:[10.1016/S0167-8809\(00\)00229-2](https://doi.org/10.1016/S0167-8809(00)00229-2)